Dalton Transactions

Accepted Manuscript

ROYAL SOCIETY OF CHEMISTRY

www.rsc.org/dalton

Structural, magnetic, and electrochemical properties of the high pressure form of $Na_2Co[PO_4]F$

Hamdi Ben Yahia[a,*], Daisuke Mori[b], Masahiro Shikano[a,*], Hironori Kobayashi[a], Yoshiyuki Inaguma[b]

Received (in XXX, XXX) Xth XXXXXXXXX 2011, Accepted Xth XXXXXXXXX 20XX
DOI: 10.1039/b000000x

The new compound HP-$Na_2Co[PO_4]F$ was synthesized by high pressure solid state reaction and its crystal structure was determined from single crystal X-ray diffraction data. The physical properties of HP-$Na_2Co[PO_4]F$ were characterized by magnetic susceptibility, specific heat capacity, galvanometric cycling, and electrochemical impedance spectroscopy measurements**.** HP-$Na_2Co[PO_4]F$ crystallizes with the space group $P6_3/m$, a = 10.5484(15), c = 6.5261(9) Å, V = 628.87(15) Å^3 and Z = 6. The crystal structure consists of infinite chains of edge-sharing CoF_2O_4 octahedra. The latter are interconnected through the PO_4 tetrahedra forming a 3D-$Co[PO_4]F$-framework. The six coordinated sodium atoms are distributed over three crystallographic sites (2*b*, 6*h*, and 4*f*). The structure of HP-$[Na1_{1/3}Na2_{3/3}Na3_{2/3}]Co[PO_4]F$ is similar to $[Na1_{1/3}Na2_{3/3}Sr_{1/3}\square_{1/3}]Ge[GeO_4]O$. There is only one difference; Na3 occupies the 4*f* (1/3, 2/3, 0.0291) atomic position, whereas the Sr occupies the 2*c* (1/3, 2/3, 1/4) atomic position. The magnetic susceptibility follows a Curie-Weiss behavior above 50 K with Θ = -21 K indicating predominant antiferromagnetic interactions. The specific heat capacity and magnetization measurements show that HP-$Na_2Co[PO_4]F$ undergoes a three-dimensional magnetic ordering at T_N = 11.0(1) K. The ionic conductivity σ, estimated at 350 °C, is 1.5 10^{-7} S cm^{-1}. The electrochemical cycling indicates that only one sodium ion could be extracted during the first charge in Na half-cell; however, the re-intercalation was impossible due to a strong distortion of the structure after the first charge to 5.0 V.

1. Introduction

Polyanionic compounds have attracted much attention during the last decades due to their potential use as the positive electrode in lithium or sodium-ion batteries. Several families of compounds have particularly been intensively investigated. Among them, the $AMBO_3$, $AMPO_4$, A_2MSiO_4, $AMSO_4X$, and A_2MPO_4X compounds which are perhaps the most interesting for practical applications (*A*: Li, Na; *M*: Mn-Ni; *X*: F, OH).[1-3 and ref. therein]

In our research group, we have also investigated the crystal structures and the physical properties of the A_2MPO_4X compounds. Several new phases have been discovered (LiNaCo[PO_4]F, LiNaFe[PO_4]F, $Li_2Fe[PO_4]F$, $LiNaFe_{1-x}Mn_x[PO_4]F$, and $Li_2Mg[PO_4]F$ crystallizing with the $Li_2Ni[PO_4]F$-type structure; LiNaMg[PO_4]F, LiNaNi[PO_4]F and $Na_2Ni[PO_4]F$ crystallizing with layered structures; and $Li_{2+x}Mg_{1-x}[PO_4]F_{1-x}\square_x$ (x = 1/4) crystallizing with a new-type of structure strongly related to $Na_2Mn[PO_4]F$).[4-10] All the LiNa*M*[PO_4]F (*M*: Fe-Ni) compounds order antiferromagnetically at low temperature. It has been demonstrated that these compounds are very sensitive to any volume change. For $Na_2Ni[PO_4]F$, when sodium is replaced by lithium or nickel by a larger transition metal, structural transitions are observed. They are mainly due to the tilt of the PO_4 tetrahedra, which causes the transformation of infinite chains of face-sharing octahedra to edge- or corner-sharing octahedra.[9] Since high pressure also induces volume changes, we started recently the study of its effect on the crystal structures and the physical properties of the Na_2MPO_4F (*M*: Mn-Ni) compounds.

The crystal structure, the magnetic- and the electrochemical-properties of $Na_2Co[PO_4]F$ (atmosphere pressure, AP) have been previously reported. AP-$Na_2Co[PO_4]F$ shows predominant antiferromagnetic interactions with weak ferromagnetism at low temperature.[11] In this paper, we report on the crystal structure of the high-pressure form of HP-$Na_2Co[PO_4]F$ which has been solved from single crystal X-ray diffraction (XRD) data. The magnetic and the electrochemical properties were also studied.

2. Experimental Section

2.1. Synthesis

A powder sample of AP-$Na_2Co[PO_4]F$ was prepared by direct solid state reaction from stoichiometric mixtures of NaF and α-$NaCoPO_4$; α-$NaCoPO_4$ was obtained by heating a 1:2:2 mixture of Na_2CO_3, $(CH_3COO)_2Co.4H_2O$ and $(NH_4)H_2PO_4$ at 350 °C for 6 h and at 750 °C for 12 h. The mixture was ground in an agate mortar, pelletized and heated at 600 °C for 12 h in a platinum crucible under air. The resulting powder was ground and fired again at 600 °C for 12 h. The progress of the reaction was followed by powder XRD. About 50 mg of the pure sample was then sealed in a gold capsule and placed in the high-pressure cell. The sample was fired at 600 °C for 30 min under a pressure of 3 GPa with a cubic multi-anvil high-pressure apparatus (NAMO2001, TRY engineering). The details are described in our previous work.[12, 13] This led to the major phase HP-

*,[a]*Research Institute for Ubiquitous Energy Devices, National Institute of Advanced Industrial Science and Technology (AIST), 1-8-31 Midorigaoka, Ikeda, Osaka 563-8577, Japan. Fax: +81-72-751-9609; Tel: +81-72-751-7932;E-mail:benyahia.hamdi@aist.go.jp, shikano.masahiro@aist.go.jp.[b] Gakushuin University, 1-5-1 Mejiro, Toshima-ku, Tokyo 171-8588, Japan*

† Electronic Supplementary Information (ESI) available: See DOI: 10.1039/b000000x/

$Na_2Co[PO_4]F$ besides a neglectable amount of an unidentified impurity. It is worth to mention that the powder contained a few tiny single crystals and the sample's color was transformed under pressure from violet to pink (Fig. 1). Under a pressure of 7.5 GPa the sample decomposes to a mixture of α-$NaCoPO_4$ and NaF, which is somewhat strange since in general a higher density phase is more stable under high pressure. The calculated density of HP-$Na_2Co(PO_4)F$ is greater than the average density of α-$NaCoPO_4$[14] and NaF.[15] The elastic property of $NaCoPO_4$ expected from bulk modulus of $Na_{4.5}FeP_2O_8(O, F)$[16] (46 GPa) and iron phosphate glasses[17] (46-48 GPa) is similar to that of NaF[18] (47.8 GPa), although the bulk modulus of $NaCoPO_4$ has not been reported. These units suggest that $NaCoPO_4$ also has a high-pressure phase with higher density than α-$NaCoPO_4$. HP-$NaCoPO_4$ stable at 7.5 GPa is unquenchable and transforms to the α-phase with pressure release. The XRD pattern of the sample prepared under the high pressure of 7.5 GPa shows larger FWHM than the one prepared under 3 GPa, which indicates a lower crystallinity.

Fig. 1. Colors of $Na_2Co[PO_4]F$ samples prepared under atmospheric pressure (left), and 3 GPa (right).

2.2. Electron microprobe analysis

Semiquantitative energy dispersive X-ray spectrometry (EDX) analyses of the powder and different single crystals including the one investigated on the diffractometer were carried out with a JSM-500LV (JEOL) scanning electron microscope (Fig. S1). The experimentally observed compositions were close to the ideal one $Na_2Co[PO_4]F$.

2.3. Powder X-Ray diffraction measurements

To ensure the purity of HP-$Na_2Co[PO_4]F$ powder, high precision powder XRD measurements were performed. The data were collected at room temperature over the 2θ angle range of $8\ ^\circ \le 2\theta \le 118\ ^\circ$ with a step size of $0.005\ ^\circ$ with a RINT-TTR diffractometer (Rigaku) operating with Cu$K\alpha$ radiations. Full pattern matching refinement was performed with the Jana2006 program package (Fig. 2).[19] The background was estimated by a Legendre function, and the peak shapes were described by a pseudo-Voigt function. The refinement of peak asymmetry was performed with four Berar-Baldinozzi parameters. The impurity peaks have been considered as excluded regions. Evaluation of these data revealed the refined cell parameters a = 10.54608(2), c = 6.52435(3) Å and V = 628.419(3) Å^3, in good agreement with the single crystal data listed in Table1.

Table 1. Crystallographic data and structure refinement for HP-$Na_2Co[PO_4]F$.

Chemical formula	HP-$Na_2Co[PO_4]F$
Crystal color	pink
Crystal size mm	0.060×0.030×0.025
M, g mol^{-1}	218.9
Crystal system	Hexagonal
Space group	$P6_3/m$
a, Å	10.5484 (15)
c , Å	6.5261 (9)
V, Å^3	628.87 (15)
Z	6
Density calcd., g cm^{-3}	3.47
Temperature, K	293(1)
$F(000)$, e	630
Diffractometer	SMART APEX
Monochromator	graphite
Radiation Å	MoKα , 0.71069
Scan mode	multi-scan
$h\ k\ l$ range	$-13 \le h \le 10$, $-13 \le k \le 10$, ± 8
$\theta_{min}, \theta_{max}$, °	2.23, 27.93
Linear absorption coeff., mm^{-1}	4.61
Absorption correction	multi-scan
T_{min}/T_{max}	0.752/0.917
No. of reflections	3491
No. of independent reflections	523
Reflections used [$I \ge 3\sigma(I)$]	364
R_{int}	0.051
Refinement	F^2
No. of refined parameters	52
R factors $R(F)$ / $wR(F^2)$	0.0349/0.0727
g. o. f.	1.20
Weighting scheme	$w = 1/(\sigma^2(I) + 0.0009I^2)$
Diff. Fourier residues, e^- Å^{-3}	-0.76/ +0.70

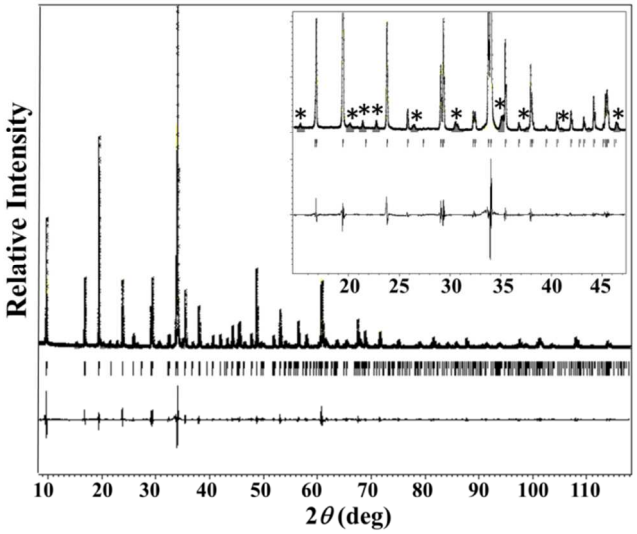

Fig. 2. Final observed, calculated and difference plots for powder XRD (Cu$K\alpha$) refinement of HP-$Na_2Co[PO_4]F$. The asterisk in the inset corresponds to an unidentified impurity. The inset corresponds to a zoom of the $2\theta = 15$ to $50\ ^\circ$ area.

2.4. Single crystal X-ray diffraction measurements

Single crystals of HP-$Na_2Co[PO_4]F$ suitable for XRD were selected on the basis of the size and the sharpness of the diffraction spots. The data collections were carried out on a Smart Apex diffractometer using MoK**α** radiation. Data processing and all refinements were performed with the Jana2006 program package.[19] A multi-scan-type absorption correction was applied with SADABS program.[20] For data collection details, see Table 1.

2.5. Magnetic susceptibility and heat capacity measurements

Magnetic susceptibility measurements of HP-$Na_2Co[PO_4]F$ were carried out with a SQUID magnetometer (Quantum Design

Magnetic Properties Measurement System (MPMS)). The susceptibility was recorded in the zero field-cooled (ZFC) and field-cooled (FC) modes over the temperature range 5–300 K under a magnetic field of 1.0 kOe. Magnetization data as a function of field were collected up to ± 10.0 kOe at 5 K after zero field cooling. Heat capacity measurements were performed with a Quantum Design PPMS (Physical Properties Measurement System) over the temperature range 2-300 K.

2.6. Electrochemical impedance spectroscopy

A.c. impedance measurements were carried out with a Solartron 1260 covering the frequency range 10^{-1}-10^{7} Hz with an applied voltage of 100 mV. Prior to measurements, the pellet was coated with Au. The sample was measured over the temperature range 20-350 °C, with equilibration periods of 30 min at each temperature. The total conductivity value for HP-$Na_2Co[PO_4]F$, corrected for pellet geometry, was calculated from the intercept of the low-frequency electrode-spike on the real axis of the complex impedance plane plot. A semicircle could be observed only at 350 °C leading to an ionic conductivity σ of 1.5 10^{-7} S cm^{-1}. The pellet was 86% dense (3.006×100/3.47).

2.7. Electrochemical cycling

Positive electrodes were made from mixtures of HP-$Na_2Co[PO_4]F$ powder, acetylene black (AB) and Polytetrafluoroethylene (PTFE) in a weight ratio of 62:30:8. The resulting electrode film was pressed with a twin roller, cut into a round plate (Φ = 14 mm) and dried at 110 °C for 12 h under vacuum. HP-$Na_2Co[PO_4]F/LiPF_6$+EC+DMC/Li and HP-$Na_2Co[PO_4]F/NaClO_4$+PC/Na coin-type cells (CR2032) were assembled in an argon-filled glove box with polypropylene as separator. Galvanometric cycling tests (CC mode) were performed in a BTS2003H (Nagano Co., Ltd) battery tester system in the potential range of 1.5–4.8 V or 1.5–5.0 V at a rate of *C*/50.

3. RESULTS AND DISCUSSION

3.1. Structure refinement

The crystal structure was initially solved from powder XRD data with EXPO2013 program.[21] The cell parameters could be determined with ito and treor programs.[22, 23] The structural model was then confirmed from single-crystal XRD data. The extinction conditions observed for the HP-$Na_2Co[PO_4]F$ single crystal agree with the $P6_3$, $P6_3/m$, $P6_3/mmm$ space groups. Most of the atomic positions were located by using the Superflip program implemented in the Jana2006 program package ($P6_3/m$ was used). The use of difference-Fourier synthesis allowed us to localize the remaining oxygen atomic positions. The fluorine and oxygen atomic positions could be distinguished by using bond-valence sum calculations (BVS). With anisotropic displacement parameters (ADPs), the residual factors converged to the values listed in Table 1. The refined atomic positions and anisotropic ADPs are given in Table 2 and S1, respectively. Inspection of the data bases revealed the structural relationship with $Na_4SrGe_3[GeO_4]_3O_3$~$[Na_{4/3}Sr_{1/3}\square_{1/3}]Ge[GeO_4]O$.[24] Further details on the structure refinement may be obtained from the Fachinformationszentrum Karlsruhe, D-76344 Eggenstein-Leopoldshafen (Germany), by quoting the Registry No. CSD–427316 for HP-$Na_2Co[PO_4]F$.

3.2. Crystal structure

HP-$Na_2Co[PO_4]F$ crystalizes with a structure very similar to $[Na_{4/3}Sr_{1/3}\square_{1/3}]Ge[GeO_4]O$ (Fig. 3a).[24] The crystal structure consists of infinite chains of edge-sharing CoF_2O_4 octahedra running along [001](Fig. 3b). The latter are interconnected through the PO_4 tetrahedra forming a 3D-$Co[PO_4]F$ framework. The six coordinated sodium atoms are distributed over three crystallographic sites (Fig. 3c-e). The $Na1O_6$ octahedra share faces and form infinite chains running along [001](Fig. 3c). The $Na2FO_5$ polyhedra share corners and form trimer units (Fig. 3d), whereas the $Na3F_3O_3$ trigonal antiprisms share faces and form dimer units (Fig. 3e). The interatomic distances and the BVS are given in Table 3.

The CoF_2O_4 octahedra are distorted with the Co-*X* distances ranging from 2.009 to 2.150 Å with an average distance of 2.097 Å. This value is very similar to that observed in LiNa$Co[PO_4]F$ (<Co1-*X* > = 2.0914 Å and <Co2-*X*> = 2.0949 Å) and in $Li_2Co[PO_4]F$ (<Co1-*X* > = 2.125 Å and <Co2-*X*> = 2.043 Å).[5, 25] It is worth noticing that in the latter two compounds, infinite chains of edge-sharing octahedra, similar to those in HP-$Na_2Co[PO_4]F$, were observed. However, the CoF_2O_4 and PO_4 polyhedra form six- and eight-membered rings in HP-$Na_2Co[PO_4]F$ (S.G.: $P6_3/m$) and LiNa$Co[PO_4]F$ (S.G.: *Pnma*), respectively (Fig.4).

Table 2. Atomic positions and isotopic displacement parameters (Å^2) for HP-$Na_2Co[PO_4]F$.

Atom	Wyck.	Symm.	*x*	*y*	*z*	*Ueq* (*Å^2*)
Na1	2*b*	-3..	0	0	0	0.0199(13)
Na2	6*h*	m..	0.1699(3)	0.3149(3)	1/4	0.0188(12)
Na3	4*f*	3..	1/3	2/3	0.0291(5)	0.0180(10)
Co	6*g*	-1	1/2	0	0	0.0100(4)
P	6*h*	m..	0.82152(17)	0.19138(18)	1/4	0.0089(6)
O1	6*h*	m..	0.6520(5)	0.0928(5)	1/4	0.0136(18)
O2	12*i*	1	0.8622(3)	0.2868(3)	0.4437(5)	0.0134(13)
O3	6*h*	m..	0.8972(5)	0.1007(5)	1/4	0.017(2)
F	6*h*	m..	0.3792(4)	0.8617(4)	1/4	0.0130(15)

Table 3. Interatomic distances (in Å), and bond valences (B.V.) for HP-$Na_2Co[PO_4]F$. Average distances are given in brackets.

	distance	B.V.
Na1-O3 (×6)	2.474(5)	0.163
	<2.474>	0.978 [a]
Na2-F	2.321(7)	0.175

Na2-O2 (×2)	2.330(3)	0.241
Na2-O3	2.434(7)	0.182
Na2-O3	2.623(4)	0.109
Na2-O1	2.700(8)	0.089
	<2.456>	1.037 [a]
Na3-F (×3)	2.356(4)	0.160
Na3-O2 (×3)	2.412(4)	0.193
	<2.384>	1.059 [a]
Na3-Na3	2.883(5)	
Co-O2 (×2)	2.009(5)	0.425
Co-F (×2)	2.1340(19)	0.270
Co-O1 (×2)	2.150(3)	0.290
	<2.097>	1.970 [a]
P-O3	1.521(7)	1.296
P-O2 (×2)	1.537(3)	1.241
P-O1	1.555(4)	1.182
	<1.537>	4.960 [a]

[a] bond valence sum, B.V. = $e^{(r0-r)/b}$ with the following parameters: b = 0.37, r_0 (P^V–O) = 1.617, r_0 (Na^I–O) = 1.803, r_0 (Na^I–F) = 1.677, r_0 (Co^{II}–F) = 1.649 Å, and r_0 (Co^{II}–O) = 1.692 Å.[26, 27]

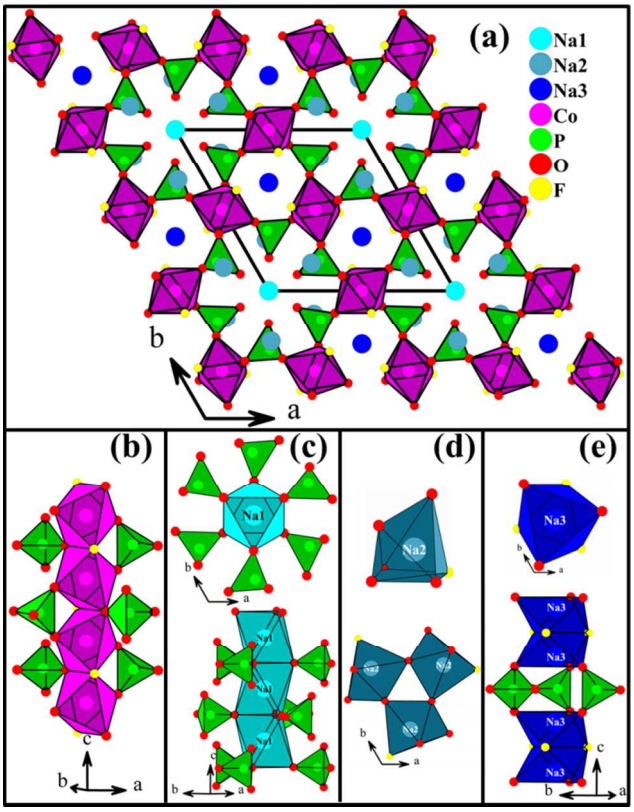

Fig. 3. Views along [001] of the crystal structure of HP-$Na_2Co[PO_4]F$ (a), and the environment of the cations; Co (b), Na1 (c), Na2 (d), and Na3 (e).

The $Na1O_6$ octahedra are highly symmetric with six equal Na1-O distances of 2.474 Å. This value is slightly higher than the expected value of 2.42 Å estimated from the effective ionic radii of the six-coordinated Na^+ and O^{2-}.[28] Such a Na environment occurs also in the homologous compound $P6_3/m$-$[Na_{4/3}Sr_{1/3}\square_{1/3}]Ge[GeO_4]O$ (2.458 Å × 6) or in $P6_3/mmc$-Na_2CO_3 (2.439 Å × 6).[24, 29] In the $Na2FO_5$ polyhedra, the Na2-X distances range from 2.321 to 2.700 Å with an average value of 2.456 Å. However, in the $Na3F_3O_3$ trigonal antiprisms the Na3-X distances range from 2.356 to 2.412 Å with an average value of 2.384 Å. Although the Na3 atoms are located in tunnels running along [001] similarly to the Sr atoms in $[Na_{4/3}Sr_{1/3}\square_{1/3}]Ge[GeO_4]O$, the two atoms do not have the same environment. Indeed, Na3 occupies the 4*f* (1/3, 2/3, 0.0291) atomic position, whereas the Sr occupies the 2*c* (1/3, 2/3, 1/4) atomic position. This is the main difference between the structures of HP-$Na_2Co[PO_4]F$ and $[Na_{4/3}Sr_{1/3}\square_{1/3}]Ge[GeO_4]O$ compounds. The BVS calculations led to 0.978, 1.037, 1.059, 1.970, 4.960, and 1.024 which are in good agreement with the values expected for $Na1^+$, $Na2^+$, $Na3^+$, Co^{2+}, P^{5+} and F^-, respectively.[26, 27]

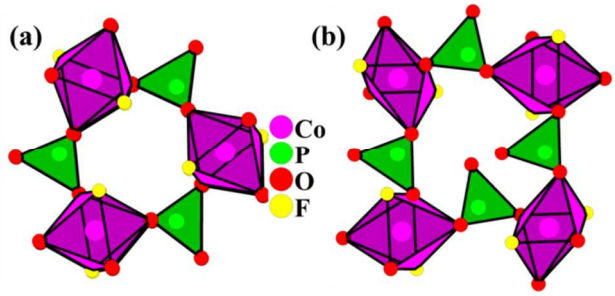

Fig. 4. Views of the six- and eight-membered-rings occurring in HP-$Na_2Co[PO_4]F$ (a) and $LiNaCo[PO_4]F$(b), respectively.

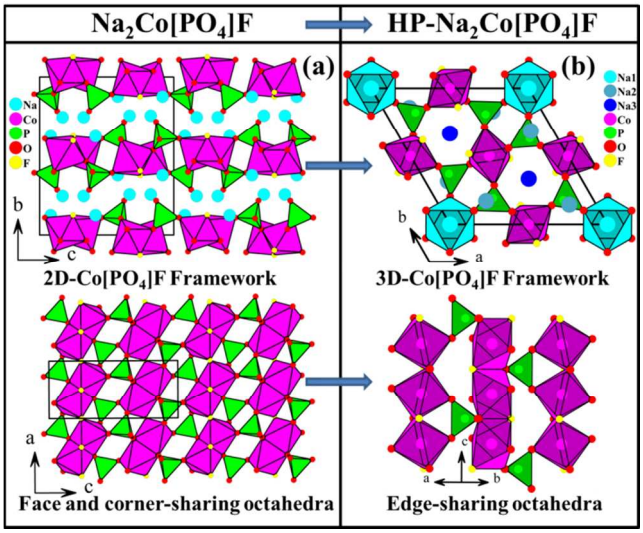

Fig. 5. Comparison of the structures of $Na_2Co[PO_4]F$ before (a), and after high pressure and temperature synthesis (b).

This study reveals that under high temperature and pressure, the layered compound AP-$Na_2Co[PO_4]F$ is transformed to a 3D-framework. More precisely, the infinite chains of dimer units (face-sharing octahedra) sharing corners are transformed to infinite chains of edge-sharing octahedra (Fig. 5), which confirms again the sensitivity of the A_2MPO_4X structures to volume changes.

It is worth noticing that $Na_5Al[PO_4]_2F_2$ and $Na_5Cr[PO_4]_2F_2$ crystallize with *P*-3 and *P*3 space groups, respectively, which are subgroups of $P6_3/m$.[30, 31] When the chemical formula are rewritten as *P*-3-$Na_2(Na_{1/2}Al_{1/2})[PO_4]F$ and *P*3-$Na_2(Na_{1/2}Cr_{1/2})[PO_4]F$, the relationship with $P6_3/m$-$Na_2Co[PO_4]F$ becomes obvious. Indeed, since the divalent cobalt cations are replaced by mixtures of trivalent and monovalent cations, the symmetry is decreased from $P6_3/m$ to *P*-3 or *P*3. During the transformation from $P6_3/m$-$Na_2Co[PO_4]F$ to *P*-3-$Na_2(Na_{1/2}Al_{1/2})[PO_4]F$, the 6*g* (Co) is splitt into 3*e* (Al) and 3*f* (Na) atomic positions, and during the transformation from *P*-3-$Na_2(Na_{1/2}Al_{1/2})[PO_4]F$ to *P*3-$Na_2(Na_{1/2}Cr_{1/2})[PO_4]F$, the 3*e* (Al)

and 3*f* (Na) are transformed to 3*d*(Cr) and 3*d*(Na) atomic positions, respectively.

3.3. Magnetic susceptibility and heat capacity measurements

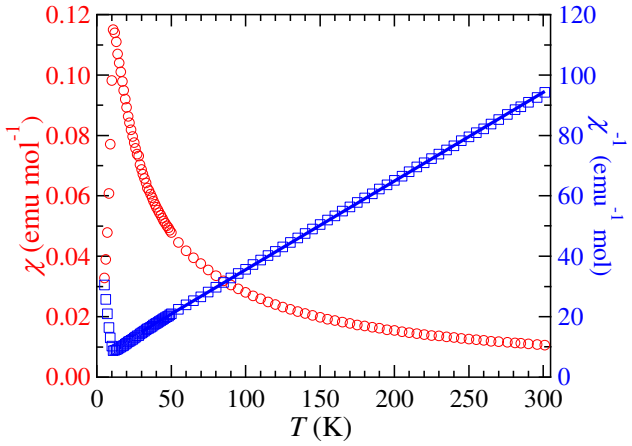

Fig. 6. Magnetic susceptibility χ vs. Temperature T and the corresponding χ^{-1} vs. T plots of HP-$Na_2Co[PO_4]F$ measured with the applied field H = 1 kOe.

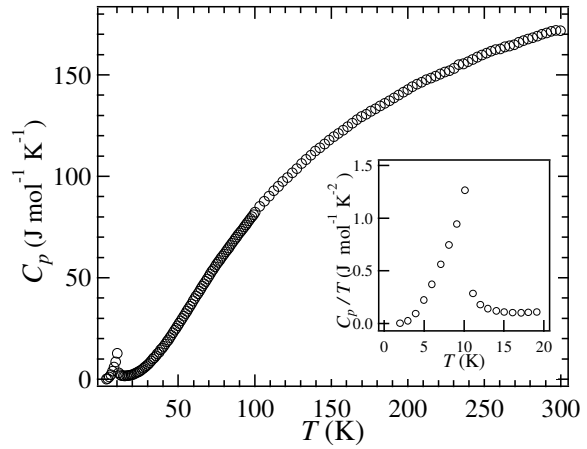

Fig. 7. Temperature dependence of the specific heat capacities C_p of HP-$Na_2Co[PO_4]F$. The inset displays C_p/T in the region of the phase transition at 11.0 (1) K.

The magnetic susceptibility χ vs. temperature T and the corresponding χ^{-1} vs. T for HP-$Na_2Co[PO_4]F$ are shown in Fig. 6. The χ^{-1} vs. T plot reveals that HP-$Na_2Co[PO_4]F$ exhibits a paramagnetic behavior in the temperature range 50 – 300 K. The susceptibility above 50 K follows a Curie-Weiss law, $\chi = C/(T-\Theta)$, with Θ = –21 K and C = 3.40 emu mol^{-1} K. The effective magnetic moment μ_{eff} calculated from the Curie constant 5.22 μ_B is a typical value obtained for divalent cobalt atoms, although higher than the spin only value of 3.87 μ_B expected for a high-spin Co^{2+} (d^7) ion, due to a contribution from the orbital angular momentum. Comparing to AP-$Na_2Co[PO_4]F$, the HP-$Na_2Co[PO_4]F$ form shows no weak ferromagnetism at low temperature.[11] Furthermore, no divergence between the ZFC and FC susceptibilities have been observed in the whole temperature range 5 − 300 K and no hysteresis has been observed on the magnetization curve at 5 K (Fig. S5).

Fig. 7 shows the temperature dependence of the specific heat capacity (C_p) and the specific heat divided by temperature (C_p/T) for HP-$Na_2Co[PO_4]F$. A λ anomaly indicating the long-range magnetic ordering of Co^{2+} ions is found at 11.0 (1) K, which corresponds to the result of the magnetic susceptibility measurements.

3.4. Electrochemical properties

The electrochemical behavior of the HP-$Na_2Co[PO_4]F$ material is depicted on the Fig. 8. When the sample was charged to 5.0 V in Na-halfcell, a charge capacity of 125 mAh/g was observed, which suggests that one sodium ion could be extracted (theoretical capacity = 122 mAh/g). During the first discharge, no Na ions could be intercalated into the structure. Consequently, the EDX analyses performed after the first charge and after five cycles indicated identical compositions which are close to $NaCo[PO_4]F$ (Fig. S2). The XRD analysis of the positive electrode (after 5 cycles) has shown a strong distortion of the structure; since the symmetry decreased from hexagonal (a = 10.5484(15), c = 6.5261(9) Å, V = 628.87(15) Å^3) to monoclinic (a = 10.6770(4), b = 6.2490(1), c = 10.5555(1) Å, β = 120.010(2) °, V = 609.86(2) Å^3). The crystal structure of the phase could not be solved due to the poor quality of the powder pattern. Perhaps, further investigation using both transmission electron microscopy and synchrotron radiation would help to solve the structure of $NaCo[PO_4]F$.

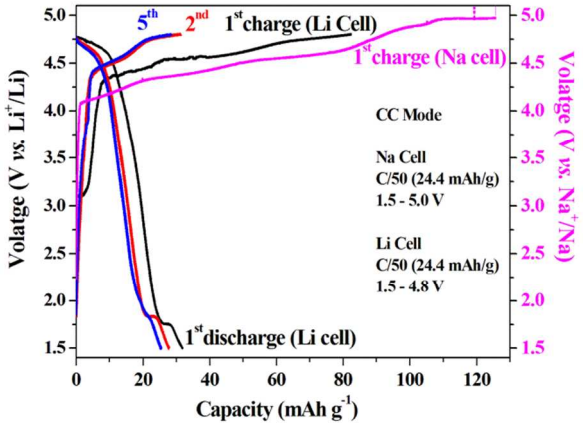

Fig. 8. Discharge/Charge curves of HP-$Na_2Co[PO_4]F$ recorded at room temperature, between 1.5 V and 4.8V vs. Li^+/Li, in a CC mode (C/50) and charge curve up to 5.0 V vs. Na^+/Na, in a CC mode (C/50).

When the sample was charged to 4.8 V in a Li-ion halfcell, a charge capacity of 80 mAh/g was observed, which suggests that approximately 0.8 sodium ions could be extracted. During the first discharge, only a capacity of 30 mAh/g was obtained. The EDX analyses performed after twelve cycles indicated compositions close to $Na_{1.3}Li_{0.7-x}Co[PO_4]F$ (x < 0.7) (Fig. S3). The XRD analysis of the positive electrode (after 12 cycles) has shown no structure distortion; however, the cell parameters decreased from (a = 10.5484(15), c = 6.5261(9) Å, V = 628.87(15) Å^3) to (a = 10.5224(1), c = 6.2791(1) Å, V = 602.09(1) Å^3) (Fig. S4).

4. Conclusion

This work reports the effect of high pressure synthesis on the crystal structure of a fluorophosphate compound with the general formula A_2MPO_4X. Indeed, under high temperature and pressure, the layered compound AP-$Na_2Co[PO_4]F$ transforms to a 3D-framework. During this transformation, the infinite chains of dimer units (face-sharing octahedra) sharing corners transform to

infinite chains of edge-sharing octahedra. The magnetic susceptibility and the specific heat measurements indicate predominant antiferromagnetic interactions with a long-range antiferromagnetic ordering at T_N = 11.0 (1) K. The electrochemical measurements indicate that HP-$Na_2Co[PO_4]F$ is active in Na and Li cells, however the performances fall short of practical application. The high pressure forms of the $Na_2Mn[PO_4]F$ and $Na_2Fe[PO_4]F$ compounds have been also investigated and will be reported in forthcoming contributions.

Acknowledgments

We thank Dr. K. Hiraki and Prof. T. Takahashi for their experimental support for the magnetic susceptibility and heat capacity measurements. Part of this work was supported by Grant-in-Aid for the Japan Society for the Promotion of Science (JSPS) Fellows Grant Number 24•02506.

References

1 G. Rousse, J. M. Tarascon, *Chem. Mater.*, 2014, **26**, 394.
2 Z. Gong, Y.Yang, *Energy Environ. Sci*., 2011, **4**, 3223.
3 C. Masquelier, L. Croguennec, *Chem. Rev.*, 2013, **113**, 6552.
4 H. Ben Yahia, M. Shikano, K. Tatsumi, S. Koike, H. Kobayashi, *Dalton Trans*., 2012, **41**, 5838.
5 H. Ben Yahia, M. Shikano, S. Koike, K. Tatsumi, H. Kobayashi, H. Kawaji, M. Avdeev, W. Miiller, C.D. Ling, J. Liu, M.-H. Whangbo, *Inorg. Chem*., 2012, **51**, 8729.
6 H. Ben Yahia, M. Shikano, H. Sakaebe, S. Koike, M. Tabuchi, H. Kobayashi, H. Kawaji, M. Avdeev, W. Miiller, C.D. Ling, *Dalton Trans*., 2012, **41**, 11692.
7 H. Ben Yahia, M. Shikano, S. Koike, H. Sakaebe, M. Tabuchi, H. Kobayashi, *J. Power Sources*, 2013, **244**, 87.
8 H. Ben Yahia, M. Shikano, H. Sakaebe, H. Kobayashi, *Mater. Chem. Phys*., 2013, **141**, 52.
9 H. Ben Yahia, M. Shikano, H. Kobayashi, M. Avdeev, S. Liu, C. D. Ling, *Dalton Trans.*, 2014, **43**, 2044.
10 H. Ben Yahia, M. Shikano, T. Takeuchi, H. Kobayashi, M. Itoh, *J. Mater. Chem. A*, 2014, **2**, 5858.
11 F. Sanz, C. Parada, C. R. Valero, *J. Mater. Chem.* 2001, **11**, 208.
12 D. Mori, M. Shimoi, Y. Kato, T. Katsumata, K. Hiraki, T. Takahashi, Y. Inaguma, *Ferroelectrics*, 2011, **414**, 180.
13 Y. Inaguma, K. Tanaka, T. Tsuchiya, D. Mori, T. Katsumata, T. Ohba, K. Hiraki, T. Takahashi, H. Saitoh, *J. Am. Chem. Soc*., 2011, **133**, 16920.
14 R. Hammond, J. Barbier, *Acta Crystallogr.*, 1996, **B52**, 440.
15 P. Debye, P. Scherrer, *Phys. Z.*, 1918, **19**, 474.
16 B. Maximov, M. Sirota, S. Werner, H. Schulz, *Acta Crystallogr.*, 1999, **B55**, 259.
17 K. H. Chang, T. H. Lee, L. G. Hwa, *Chinese J. Phys.*, 2003, **41**, 414.
18 T. Yagi, T. Suzuki, S. Akimoto, *J. Phys. Chem. Solids*, 1983, **44**, 135.
19 V. Petricek, M. Dusek, L. Palatinus, Jana2006, *The crystallographic computing system*, Institute of Physics, Praha (Czech Republic) 2006.
20 Bruker (2001). SADABS. Bruker AXS Inc., Madison, Wisconsin, USA.
21 A. Altomare, C. Cuocci, C. Giacovazzo, A. Moliterni, R. Rizzi, N. Corriero and A. Falcicchio, "EXPO2013: a kit of tools for phasing crystal structures from powder data", *J. Appl. Cryst.*, 2013, **46**, 1231.
22 P.-E. Werner, L. Eriksson, M. Westdahl , TREOR, a Semi-Exhaustive Trial-and-Error Powder Indexing Program for All Symmetries, *J. Appl. Cryst.,* 1985, **18**, 367.
23 J. W. Visser, A Fully Automatic Program for Finding the Unit Cell from Powder Data, *J. Appl. Cryst.*, 1969, **2**, 89.
24 T.N. Nadezhina, E.A. Pobedimskaya, N.V. Belov, *Sov. Phys. Crystallogr.* (Engl. Transl.) 1975, **19**, 536.
25 J. Hadermann, A. M. Abakumov, S. Turner, Z. Hafideddine, N. R. Khasanova, E. V. Antipov, G.V. Tendeloo, *Chem. Mater.*, 2011, **23**, 3540.
26 I. D. Brown, D. Altermatt, *Acta Crystallogr.*, 1985, **B41**, 244.
27 N. E. Brese, M. O'Keefe, *Acta Crystallogr.*, 1991, **B47**, 192.
28 R. D. Shannon, *Acta Crystallogr*., 1976, **A32**, 751.
29 I. P. Swainson, M. T. Dove, M. J. Harris, *J. Phys. Condens. matter*, 1995, **7**, 4395.
30 J. Arlt, M. Jansen, H. Klassen, G. Schimmel, G. Heymer, *Z. Anorg. Allg. Chem.*, 1987, **547**, 179.
31 P.G. Nagornyi, A.A. Kapshuk, Z.I. Kornienko, V.V. Mitkevich, S.M.' Tret, *Russ. J. Inorg. Chem.*, 1990, **35**, 470.

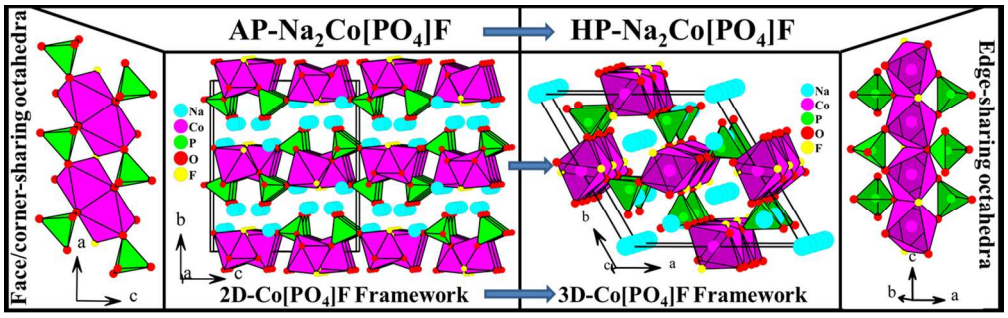

The high pressure form of Na2Co[PO4]F
282x87mm (150 x 150 DPI)